Using NOMA for Enabling Broadcast/Unicast Convergence in 5G Networks

Eneko Iradier, *Student Member, IEEE*, Jon Montalban, *Member, IEEE*, Lorenzo Fanari, *Student Member, IEEE*, Pablo Angueira, *Senior Member, IEEE*, Liang Zhang, *Senior Member, IEEE*, Yiyan Wu, *Fellow, IEEE*, and Wei Li, *Member, IEEE*

***Abstract*—This paper addresses the challenge of broadcast and unicast convergence by proposing a PHY/MAC (Physical Layer/Medium Access Control) architecture for 5G New Radio (NR). The solution is based on Power domain Non Orthogonal Multiple Access (P-NOMA). The main PHY/MAC configuration parameters have been analyzed theoretically and their impact on the service configurations is presented in this manuscript. The system concept has been translated into a prototype model and different evaluation tests are presented. First, simulations show that the PHY layer performs better than Time Division Multiplexing/Frequency Division Multiplexing (TDM/FDM) choices of current broadband access systems. Second, performance tests using a network simulation tool are described. The results for capacity, latency and reliability demonstrate that the proposed solution offers an excellent broadcast/unicast convergence choice with significant gain values with respect to legacy PHY/MAC alternatives.**

***Index Terms*—5G, broadcast, convergence, LDM, MAC, NOMA, P-NOMA, unicast.**

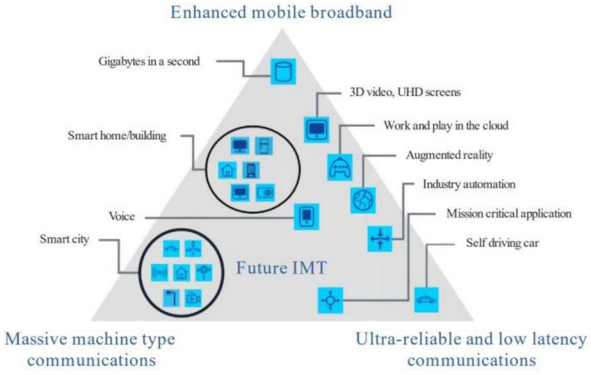

Fig. 1. 5G NR applications and use case families [3].

I. Introduction

THE STANDARDIZATION process required to create and enhance the fifth generation of mobile communications (5G), which is expected to cover all the increasing connectivity necessities [1], is ongoing. In fact, the first Release (Rel-15) of 5G has already been published, including New Radio (NR) [2], and several improvements in different levels of the protocol stack make this solution a proper alternative for different use cases. One of the most relevant contributions can be considered the development of a flexible Physical Layer (PHY) that can be implemented in several scenarios with completely different requirements. It should also be mentioned that Low-Density Parity-Check (LDPC) codes are introduced to enhance the communication reliability.

The Radiocommunication Sector of the International Telecommunication Union (ITU-R) has divided the entire application frame into three use case families: enhanced Mobile Broadband (eMBB), Ultra Reliable Low Latency Communications (URLLC) and massive Machine Type Communications (mMTC) [3]. In Fig. 1, a summary of the use case families is shown with some other more specific applications.

Each one of the different use case families shown in Fig. 1 has different requirements. In eMBB, which is related to the classic information and entertainment media delivery scenario, high data rates are required. In fact, it is expected to guarantee peak data rate values close to 10 Gbps for the uplink and 20 Gbps for the downlink and support speeds up to 500 km/h. In the case of URLLC, as it is oriented to mission-critical communications, reliability and latency are the most demanded requirements. In fact, an upper bound of one millisecond of end-to-end latency has been established in the user plane. Finally, concerning mMTC, the network is expected to increase the device density rate to values close to 10^6

Manuscript received December 1, 2019; revised March 2, 2020; accepted March 3, 2020. Date of publication April 14, 2020; date of current version June 5, 2020. This work was supported in part by the Basque Government (Project IOTERRAZ) under Grant KK-2019/00046 ELKARTEK 2019, Grant IT1234-19, and the PREDOC Grant Program PRE_2019_2_0037, and in part by the Spanish Government (Project PHANTOM) under Grant RTI2018-099162-B-I00 (MCIU/AEI/FEDER, UE). *(Corresponding author: Eneko Iradier.)*

Eneko Iradier, Jon Montalban, Lorenzo Fanari, and Pablo Angueira are with the Department of Communications Engineering, University of Basque Country (UPV/EHU), 48013 Bilbao, Spain (e-mail: eneko.iradier@ehu.eus; jon.montalban@ehu.eus; lorenzo.fanari@ehu.eus; pablo.angueira@ehu.eus).

Liang Zhang, Yiyan Wu, and Wei Li are with the Department of Wireless Communications, Communications Research Centre Canada, Ottawa, ON K2H 8S2, Canada (e-mail: liang.zhang@canada.ca; yiyan.wu@canada.ca; wei.li@canada.ca).

Color versions of one or more of the figures in this article are available online at http://ieeexplore.ieee.org.

Digital Object Identifier 10.1109/TBC.2020.2981759

devices per km^2 and increase the battery lifetime to around 10 years.

The combination of the large list of new applications and the configuration flexibility presented in the latest Release gives the opportunity to make 5G the main generic solution for wireless communications. However, a mechanism that could enhance the 5G performance is still missing: Point-to-Multipoint (PTM) communications. Although it is true that broadcast/multicast communications are not considered in this first version, they will probably be integrated in future Releases (Rel-17/18).

In parallel to the integration of PTM communications, the convergence between unicast and broadcast services is still an open issue. In 4G systems, Evolved Multimedia Broadcast Multicast Services (eMBMS) has been implemented, which is based on Time Division Multiplexing (TDM) and is complemented with Frequency Division Multiplexing (FDM).

This paper proposes a different standpoint to replace or to complement eMBMS by means of Non-Orthogonal Multiple Access (NOMA) techniques.

As described in [4], a layered division or power-based NOMA can be implemented in order to deliver simultaneously different services, assuming diverse power levels and configurations. The main advantage of P-NOMA systems is that the 100% of the RF bandwidth is used during the 100% of time to transmit two (or more) services. That is why NOMA is considered a spectral efficiency friendly technique when compared with orthogonal multiplexing access solutions, such as TDM or FDM.

The main example of the success of P-NOMA systems is the acceptance of a low complexity P-NOMA structure, Layered Division Multiplexing (LDM), to be part of the Advanced Television Systems Committee (ATSC 3.0) PHY layer baseline technology [5]. In this case, a robust configuration is implemented in the Upper Layer (UL), oriented to portable and mobile receivers. On the other hand, in the Lower Layer (LL), a high capacity configuration is chosen to deliver high data rate services, such as Ultra High Definition Television (UHDTV) or multiple High Definition Television (HDTV) services, to fixed receivers.

The main objective of this paper is to propose, design and evaluate a novel solution for enabling broadcast/unicast service convergence in 5G networks based on P-NOMA. Afterwards, the main implications of this architecture are presented as well as implementation guidelines based on a prototype. Finally, the prototype is evaluated at PHY level using an upgraded network simulation tool. PHY and network layer results are shown and analyzed, separately.

In summary, the technical contributions of this paper include:

1) Full architecture definition of a P-NOMA solution for 5G NR at PHY/MAC (Medium Access Control) level. Some blocks of the architecture are novel and critical for the overall performance of the proposal.
2) Design and implementation of a frame adaptation layer to combine UL and LL MAC packets.
3) Performance evaluation and gain analysis of the proposed technique over different propagation channels.
4) Presentation of network level simulations and reliability, latency and capacity analysis.

The rest of the paper is organized as follows. The next section describes related work published up to now on this topic. Section III is focused on overview of 5G NR at different levels. In Section IV, NOMA-based 5G model is presented, taking into account the implications and the proposed novelties. Then, in Section V, a PHY level evaluation of the proposed solution is carried out. In Section VI, the proposed solution is tested in a network simulation tool. Finally, Section VII contains the conclusions and the future works.

II. Related Work

A. Broadcast/Unicast Convergence

5G is expected to be the global wireless solution to guarantee convergence and cooperation between different networks, devices and technologies [6]. However, in its first version, Rel-15, a fundamental scenario, especially for eMBB communications, has not been considered: PTM communications.

The broadcast implementation roadmap in 5G has similar milestones when compared to 4G. Although a broadcast traffic distribution alternative was already included in 3G systems within Multimedia Broadcast Multicast Services (MBMS), it was not until Rel-9 that the first broadcast transmission capabilities were introduced. In fact, in 4G, a slightly enhanced solution was presented (evolved MBMS, eMBMS), which brought higher and more flexible data rate configurations, single frequency network (SFN) operations and carrier configuration flexibility [7]. Latest enhancements applied to eMBMS were included in Long Term Evolution (LTE) Rel-14. One of the most relevant differences was that the limitation of the maximum of 60% of radio resources for broadcast transmissions was removed [8]. In addition, support for eMBMS will be introduced for NR mainly for public safety use cases, Vehicle-to-everything (V2X) applications and railways, and therefore, further enhancements will come in Rel-16 [9].

Concerning the future of broadcast in 5G, the most relevant contributions are related to the 5G-Xcast project [10]. 5G-Xcast was an international research project, funded by the European Commission (EC) that started in June 2017. This project presented a cross-layer PTM proposal at different architecture levels. Among other contributions in 5G-Xcast project, in [11], a specific approach of the 5G NR PHY for terrestrial broadcast was presented. In this paper, the critical parameters of the waveform generation are discussed and the NR-based MBMS solution is compared with the latest LTE Rel-14 version. Aiming to cover a different perspective, in [12], the network slicing concept is discussed within the 5G paradigm. The main implications are detailed in order to optimize the network resources of a particular 5G infrastructure over different PTM use cases.

B. NOMA for 5G Systems

P-NOMA-based systems such as LDM, have demonstrated very positive spectral efficiency properties and an excellent performance for broadcast applications [4]. Nevertheless,

LDM has not been so successful for broadband communication systems and although NOMA was adopted by 3GPP Rel-14, it has not been implemented so far. However, several works presented P-NOMA-based solutions as relevant candidates for broadcasting in 5G [13]–[18].

One of the first works that evaluated the use of P-NOMA within eMBMS is reported in [13]. In this paper, several scenarios where LDM could take advantage of its efficiency increase were presented and the theoretical Signal-to-Noise Ratio (SNR) thresholds for different injection level (IL) values were provided. Some other works evaluated the theoretical interoperability of P-NOMA with the eMBMS ecosystem [14], [15]. While [14] studies the use of LDM as a key technology for 5G networks to deliver PTM transmission within the broadband systems, the authors in [15] present NOMA as a candidate to carry out multicast transmissions in subgroup oriented communications.

Concerning non-theoretical contributions, in [16], the transmission of unicast and broadcast services at the same time in a SFN by using LDM were analyzed. In this case, the study was based on measuring the power consumption per base station. The results provide power savings simultaneously for unicast and broadcast transmissions due to the larger bandwidth available. In [17], P-NOMA was proposed in combination with TDM schemes to deliver mixed broadcast and unicast services in a 5G-MBMS environment. The performance and the implications of using P-NOMA for both services, broadcast and unicast, were presented and evaluated. Results indicate that significant capacity gains could be achieved when using P-NOMA in 5G NR. However, the only Key Performance Indicator (KPI) evaluated is capacity, while latency and reliability are not taken into account. Finally, in [18], the first NOMA-based 5G NR PHY layer transceiver was presented. The prototype was tested by implementing a convergence-oriented use case. Results offer significant capacity gains in different configurations. However, the AWGN channel was the only simulation case and the impact of retransmissions (Hybrid Automatic Repeat Request, HARQ) was not evaluated.

III. 5G Overview

As in 4G, 5G NR PHY is based on Orthogonal Frequency Division Multiplexing (OFDM) technique. However, one of the main novelties of this standard is not the base technology, but its configuration flexibility. There are five different numerologies (μ) available with different subcarrier spacing (SCS) values obtained from the following expression:

$$SCS(kHz) = 15 \cdot 2^{\mu} \tag{1}$$

where μ represents the numerology and it can be 0, 1, 2, 3 or 4.

In NR, each radio frame has a fixed length of 10 ms and it is composed of a fixed number of ten subframes. Moreover, each subframe has a duration of one millisecond. The number of slots per subframe varies depending on the numerology that is implemented. In TABLE I, a summary of the possible number of slots per subframes and their duration is presented as a function of the numerology. In comparison with 4G, this aspect is considered a relevant difference. In addition, although the default number of symbols per slot is 14, different configurations can be implemented. On the one hand, in order to enable the transmission of short data packet, a mini-slot configuration has been introduced in the standard, where 2, 4 or 7 symbols can be allocated. On the other hand, just with the opposite aim, slots can be gathered for longer transmissions.

TABLE I
5G NR Subcarrier Spacing Influence

μ	SCS (kHz)	# Slots/Subframe	Slot (ms)
0	15	1	1
1	30	2	0.5
2	60	4	0.25
3	120	8	0.125
4	240	16	0.0625

TABLE II
OFDM Symbols

	$\mu = 0$	$\mu = 1$	$\mu = 2$	$\mu = 3$	$\mu = 4$
OFDM Symbol (μs)	66.67	33.33	16.67	8.33	4.17
CP (μs)	4.69	2.34	1.17	0.57	0.29
Total length (μs)	71.36	35.67	17.84	8.90	4.46

Another variable that can be tuned is the OFDM symbol length. TABLE II presents the OFDM symbol lengths with and without the Cyclic Prefix (CP). As shown, the shortest OFDM symbol lengths allow their transmission in less than 5μs. In consequence, the highest numerologies, especially $\mu = 3$ and $\mu = 4$, are designed to address URLLC by using shorter transmission durations.

Finally, the main PHY level novelty from the reliability point of view is the new channel coding. NR does not include Turbo-codes; LDPC and Polar codes are supported. Polar codes are reserved for control packet transmissions and LDPC codes are used in payload data packets. Indeed, LDPC codes have demonstrated to be a very robust channel coding technique and their reliability is very close to the Shannon limit, just half a dB away [19], [20].

Regarding the MAC layer implemented in NR, several characteristics have been directly inherited from LTE: the mapping process between logical and transport channels, the multiplexing/demultiplexing of MAC Service Data Units (SDU) when required, etc. Moreover, as in LTE, HARQ techniques are used for error correction. 5G NR HARQ are error correction techniques based on packet retransmissions. The main difference when compared with 4G is that the timing between data transmission and the HARQ response is flexible. While in 4G timing was fixed to 4 ms, in 5G the number of time slots between data transmission and the HARQ response can be dynamically adapted for enabling lower latencies.

Another aspect that has been modified in NR is the resource management. As shown in Fig. 2, the smallest unit that appears in the resource grid is the Resource Element (RE), which consists of one subcarrier and one OFDM symbol, in frequency and time domain, respectively. However, the Resource Block (RB) concept is not the same as in 4G. In NR, RBs are defined as 12 consecutive subcarriers in one OFDM symbol. Then, as presented in TABLE III, the minimum and

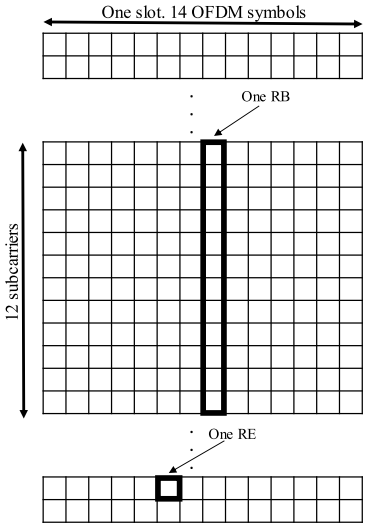

Fig. 2. Basic resource management terminologies.

TABLE III
RESOURCE BLOCKS AND BANDWIDTH SIZES

μ	RB_{MIN}	RB_{MAX}	BW_{MIN} (MHz)	BW_{MAX} (MHz)
0	24	275	4.32	49.5
1	24	275	8.64	99
2	24	275	17.28	198
3	24	275	34.56	396
4	24	138	69.12	397.44

maximum bandwidths were defined for each of the possible numerologies (from 4.32 MHz to 397.44 MHz). Finally, the amount of RBs required to obtain the bandwidth ranges was calculated according to each numerology and bandwidth range by dividing the bandwidth by the size of one RB.

IV. 5G-NOMA

In this section, the implications of introducing NOMA in the 5G PHY are presented. First, the general structure is introduced and then, several issues regarding the implementation are explained.

A. General Structure

In the first phase of this work, a transceiver has been developed in MATLAB. This prototype is partially compliant with the NR Rel-15 standard. A Physical Downlink Shared Channel (PDSCH) has been implemented in the prototype, since 5G NR does not include any specific broadcast channel for data delivery. Nevertheless, the prototype is compatible with any future broadcast channel that could be introduced in the future (Rel-17/18). In addition, in order to introduce NOMA in the 5G NR transceiver some modifications have been done. In Fig. 3, a general block diagram of the overall transceiver is shown. The blocks related to the transmitter are color coded in orange, while receiver blocks are painted in blue.

At the beginning of the transceiver, two independent data flows are created, one per each NOMA layer. The blocks related to UL are located inside the green dashed box, while the blocks related to the LL are inside the red dashed box. A Downlink Shared Channel (DL-SCH) transport channel is generated for each layer, and then, the DL-SCH is encapsulated into PDSCH, where the modulation and the LDPC coding is applied. The LDPC codeword size is adapted depending on the modulation and code rate that is used.

Once PDSCH are generated for both layers, they are combined into a single NOMA signal ensemble. Therefore, symbols corresponding to the LL are attenuated by a predefined IL (g, in Fig. 3, expressed in linear units). The IL indicates the relative power distribution between both layers, so g has a real value within the range [0, 1), where $g = 0$ results in a single-layer system and $g = 1$ results in a two-layer system with equal power distribution [4]. The IL can also be expressed in dBs (IL $= 10 \cdot \log(g)$). Then, the UL and the attenuated LL are added creating the definitive NOMA signal ensemble. After superimposing both layers, the output constellation is normalized. Finally, the precoding matrix for the next transmission is calculated using singular value decomposition (SVD). Then, the OFDM signal is generated.

The transmitted signal is filtered through the channel model block. In this case, two channel model families have been integrated: an ideal channel-fading model with Additive White Gaussian Noise (AWGN) and a Tapped Delay Line (TDL) [21]. The first will be used as a reference to test the prototype and define the PHY configurations, while the second one is implemented as a more realistic and challenging channel model. TDL channel models are defined for the full frequency range and for non-MIMO transmissions. They are composed by several taps with different delays and amplitudes. Five different channel profiles are defined, where TDL-A, TDL-B and TDL-C represent channel models for Non-Line of Sight (NLOS) conditions and TDL-D and TDL-E are aimed for Line of Sight (LOS) conditions [21]. More details are presented about the parameters of the implemented channel models in Section V.

At the receiver, the first modules perform OFDM demodulation and channel estimation. The channel estimation block also removes the precoding information form the channel estimation. Then, for UL recovery, demodulation and LDPC decoding is applied at PSDCH and DL-SCH blocks. The UL noise threshold is low and in consequence, the lower layer will be assumed as additional noise for the UL. In order to recover the LL, a Successive Interference Cancellation (SIC) module has been introduced. Since this module takes as input the received signal and the regenerated UL, the DL-SCH and the PDSCH modules have to be applied again to re-create UL bits. The output of the SIC module is the difference between both signals, i.e., the received LL. Hence, to obtain the definitive transmitted LL bits, PDSCH decoding and DL-SCH decoding is applied to the output of the SIC module.

In parallel to the complete 5G-NOMA architecture, HARQ retransmission schemes are also implemented. In this case, when the UL data and the LL data are obtained in the DL-SCH decoding module, received packets are checked. If the packet is received successfully, a new transport block is generated and transmitted. However, if errors occur, a retransmission is scheduled by changing the Redundancy Version (RV) value.

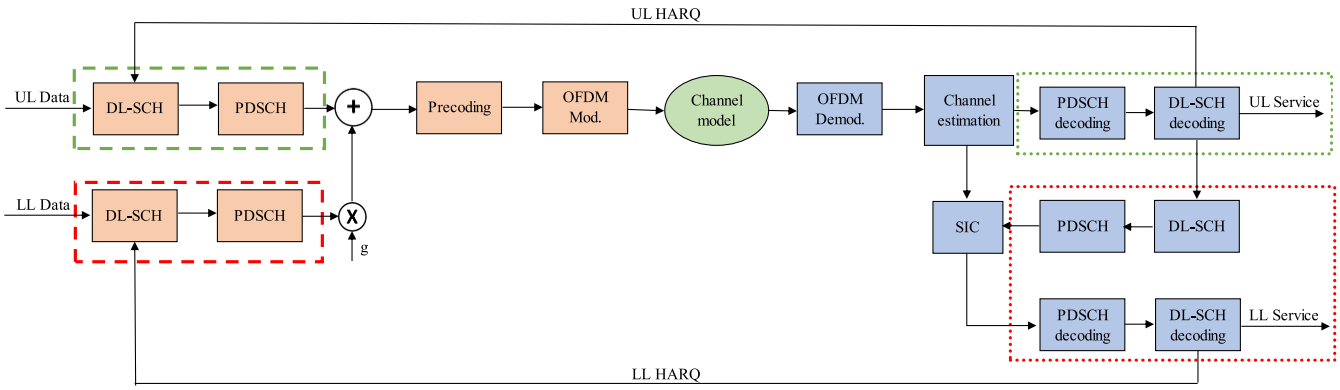

Fig. 3. Simplified general block diagram of the transceiver architecture.

In the proposed 5G NOMA implementation, HARQ processes are independently carried out in each layer.

Finally, it is important to highlight complexity aspects. It is true that introducing NOMA techniques in the 5G NR standard, the complexity of the transceiver will be increased. However, this complexity drawback does not affect the complexity of receivers only intended for the UL decoding. In fact, as it can be seen in Fig. 3, the UL decoding chain follows the traditional modules. Therefore, only the receivers interested on recovering LL suffer from extra complexity increase associated to the SIC module.

B. Frame Adaptation Layer

Although UL and LL data flows are independently configured, a joint framing management is needed. Indeed, when the NOMA signal ensemble is created, the inputs to both layers must have the same length. That is why, a new adaptation layer between the MAC and the PHY is required. The frame adaptation layer is based on the following expression:

$$\#SC_{UL} = \#SC_{LL} \tag{2}$$

where $\#SC_{UL}$ and $\#SC_{LL}$ are the number of subcarriers allocated for the transmission in the UL and in the LL, respectively. This parameter defines the amount of coded bits that can be transmitted:

$$\#\ SC_{UL} = \frac{tx\ bits_{UL}}{m_{UL}} = \frac{tx\ bits_{LL}}{m_{LL}} \tag{3}$$

where *tx bits* is the amount of bits that are introduced in the modulator and m is the modulation index. Finally, the amount of transmitted bits is calculated from the following relation:

$$\#\ SC_{UL} = \frac{info\ bits_{UL} \cdot CR_{UL}}{m_{UL}} = \frac{info\ bits_{LL} \cdot CR_{LL}}{m_{LL}} \tag{4}$$

where *info bits* are the PHY transport block bits and *CR* is the implemented code rate. Assuming a fixed amount of information bits for the UL, the amount of information bits for the LL in each frame is calculated from the following expression:

$$info\ bits_{LL} = \frac{info\ bits_{UL} \cdot CR_{UL} \cdot m_{LL}}{m_{UL} \cdot CR_{LL}} \tag{5}$$

Therefore, the length of the LL packet received from the MAC layer is restricted by the combination of the modulation order and the code rate (Modulation and Coding Scheme, MCS) of each layer and the length of the UL MAC packet.

Simulations use complete time slots so the number of subcarriers allocated for each iteration will be driven by SCS and bandwidth choices. In practice, the length of MAC packets will be then set by defining modulation and code rates of UL and LL.

C. Resource Allocation

As described in Section III, one RB is the minimum data unit that can be allocated in 5G NR. Indeed, this resource allocation technique implies frequency domain multiplexing (subcarriers) and time domain multiplexing if more than one RB is gathered. Therefore, P-NOMA can be considered a two dimensional multiplexing technique. In Fig. 4(a), an example of NR Rel-15 resource allocation pattern is shown. Each color represents the one different service or unicast receiver. However, if P-NOMA is introduced in the 5G NR resource allocation mechanism, another parameter should be taken into account when distributing the resource: the transmitted power. In Fig. 4(b), an example of a resource allocation pattern when P-NOMA is implemented is shown. Again, each color represents a different transmitted service. In this case, inside each RB due to the IL, more than one service can be delivered. Therefore, if P-NOMA is introduced in 5G NR, a three dimensional resource allocation should be carried out: time, frequency and power. Undoubtedly, this third dimension increases the number of parameters and possible pattern combinations, and, therefore, higher flexibility when applying the resource allocation.

D. Broadcast/Unicast Convergence

The resource allocation approach presented in Section IV-C presents a new alternative to cover different use cases. In fact, P-NOMA would enable the convergence between broadcast and unicast services in the same RF channel. On the one hand, Fig. 4(c) shows how the broadcast/unicast convergence issue is solved in eMBMS. As it can be seen, broadcast and unicast services are multiplexed by using frequency domain multiplexing, although a similar allocation pattern can be

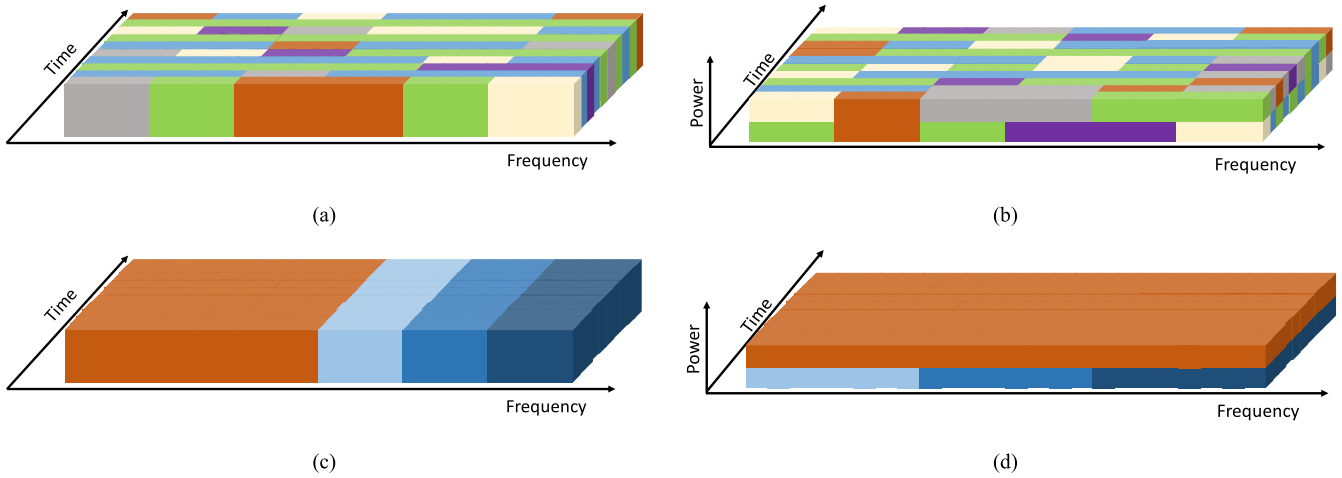

Fig. 4. Resource allocation patterns: (a) generic TDM/FDM, (b) generic P-NOMA, (c) broadcast/unicast convergence solution in TDM/FDM, (d) broadcast/unicast convergence solution in P-NOMA.

obtained if a time domain multiplexing is followed. The dark orange block represents the allocation for the broadcast service, whereas the blue blocks are reserved for different unicast services, where each blue tone represents a specific unicast service. In this case, a 50%-50% time division has been applied between broadcast and unicast services, which means that the available resources are equally shared between broadcast and unicast services. Moreover, concerning the unicast services, three simultaneous services have been assumed with an equal resource sharing among them.

On the other hand, in Fig. 4(d) the broadcast/unicast convergence issue is solved by implementing P-NOMA in the 5G NR resource allocation mechanism. As in Fig. 4(c), dark orange block represents the broadcast service and the blue blocks are different unicast services. In this case, broadcast and unicast services are sharing the same OFDM symbol and the same subcarriers, but they are superimposed with different power levels. The UL is reserved for the broadcast content, whereas the LL is used for delivering unicast services, since traditional broadcast transmissions have to guarantee a high reception rate and so, they have to meet more strict availability requirements. Then, in the LL in order to share the resources among the different unicast services frequency domain multiplexing is used. Therefore, the resource allocation scheme presented in Fig. 4(d), as in Fig. 4(b), implies LDM + FDM (or TDM) multiplexing scheme concatenation. Comparing Fig. 4(c) and 4(d), the latter certainly provides wider available bandwidth for each service, resulting in capacity gain.

When P-NOMA is used to guarantee the convergence between broadcast and unicast services, the main parameter to configure the overall content distribution is the IL. Therefore, the implemented IL value has a direct impact in the delivered services and so, a tradeoff has to be assumed between the characteristics of broadcast and unicast services. For example, if high IL values are selected, higher throughput can be obtained in the UL (or higher reliability) for the broadcast service. However, as the power reserved for the LL is lower, the available capacity will decrease, and less unicast services could be delivered. On the other hand, if low ILs are selected in order to enhance the unicast services, the reliability of the UL will be reduced and the broadcast coverage area could be noticeably impacted.

V. PHY Evaluation

This section describes the evaluation of the PHY P-NOMA solution in different propagation channels.

A. Theoretical Approach

A use case with a mixture of broadcast and unicast services has been designed. The broadcast service is 4K UHDTV content delivered on a 30 Mbps bit stream [22]. Availability will be considered a critical factor because correct reception has to be guaranteed to 99% of the receivers at least. On the other hand, in the case of the unicast services, configurations that allow higher data rates have been used. The reference value for unicast services has been set to 50 Mbps, which has to be shared among all the unicast receivers. For this kind of services, the higher the available data rate is, the higher the amount of users that could simultaneously receive the service can be. Some examples of this type of services are: Internet of Things (IoT) for smart traffic management or on demand TV content for mobile receivers.

From a multiplexing standpoint, P-NOMA offers a new dimension for system flexibility and the capacity and robustness requirements posed by each service can be tailored with different time, frequency and power domain adjustments. Examples shown in TABLE IV explain how broadcast services would be delivered in the UL and unicast services in the LL. The values in TABLE IV provide comparison metrics between the expected capacities and thresholds in P-NOMA and TDMA. Capacity is calculated for a NR signal of 20 MHz bandwidth and SNR thresholds are based on AWGN simulations.

The methodology for comparing P-NOMA and TDMA starts setting the service bitrate requirements in TDMA (30 Mbps UHDTV Broadcast content and 50 Mbps

TABLE IV
USE CASES CONFIGURATION

Service	TDMA (50%-50%)			NOMA (I) (IL = -6 dB)			NOMA (II) (IL = -6 dB)		
	MCS	Cap. (Mbps)	SNR_{TH} (dB)	MCS	Cap. (Mbps)	SNR_{TH} (dB)	MCS	Cap. (Mbps)	SNR_{TH} (dB)
Broadcast	12	30.3	11.1	5	29.5	11	5	29.5	11
Unicast	19	51.2	17.5	10	51.4	15.8	12	60.6	18

unicast capacity). The TDMA choices are MCS 12 (64QAM 517/1024 and 3.0293 bps/Hz) and MCS 19 (64QAM 873/1024 and 5.1152 bps/Hz) (according to [23, Table 5.1.3.1-2]).

Then, P-NOMA is adjusted to provide equivalent UL bitrate and robustness (4K UHDTV content). The UL MCS selection is MCS5 (16QAM 378/1024 and 1.4766 bps/Hz) while two possible variants are proposed for the lower layer. NOMA (I) optimizes the system threshold while maintaining capacity (51.4 Mbps vs. 51.2 Mbps) using a LL MCS10 (16QAM 658/1024 and 2.5703 bps/Hz). NOMA (I) configuration provides a 1.7 dB improvement in the LL with respect to the equivalent TDMA threshold. A second optimization case is NOMA (II) that maintains an equivalent threshold (18 dB) with MCS12 (64QAM 517/1024 and 3.0293 bps/Hz) and varies capacity (60.6 Mbps vs 51.2 Mbps). The injection level in P-NOMA has been set to -6 dB to guarantee that the service area of both systems is equivalent.

B. Simulation Results

Once a preliminary analysis based on the AWGN channel has been carried out, more simulations have been performed over different propagation channels in order to widen the results.

Concerning the wireless propagation channel, TDL-D and TDL-E profiles have been implemented. In both cases, the LOS condition is included. Additionally, three different desired delay spread (DDS) values have been simulated for each channel model: 90 ns, 360 ns and 1100 ns. Those values have been selected because they are aligned with short-, normal- and long-delay profiles for an urban environment [21].

Results obtained with the developed transceiver over the detailed channels are presented in Fig. 5. Following those graphics, a performance comparison can be made between P-NOMA and TDMA multiplexing schemes.

From a general perspective, each transmission configuration shows a similar performance over the different channels. In comparison with the AWGN channel, the performance is deteriorated in the range of 0.3 dB and 2 dB. The short-delay and the normal-delay profiles, present very similar results in both cases. It should be highlighted, however, that the long-delay profile channels have stronger negative effects on the received signal and the required SNR thresholds are higher. In fact, the TDL-E channel model is even more challenging in long-delay conditions than the TDL-D.

As expected, services oriented to fixed receivers (TDMA (I) and NOMA (UL)) show a very similar reliability performance. In fact, the difference between both cases, in terms of required SNR threshold for a BER value of 10^{-6}, is around 0.1 dB. However, the behavior of the BER vs SNR curve is not identical in both cases. While the TDMA case presents a very pronounced decrease, the UL case has a slower decrease. This difference is due to the NOMA configuration. The effective SNR value for the UL is close to 6 dB, due to the IL. This value is very close to the SNR threshold required to decode this configuration in the single layer mode and, in consequence, the UL is not able to offer a fast decrease. Nevertheless, this problem could be solved by increasing the IL value. In that case, the SNR value required to obtain the LL service would be higher.

TABLE V
RELIABILITY/CAPACITY GAIN ANALYSIS OF THE LL (UNICAST SERVICES)

Metric		NOMA (I)	NOMA (II)
SNR_{TH} Gain (dB)	TDL-D 90 ns	1.7	-0.4
	TDL-E 90 ns	1.7	-0.6
	TDL-D 360 ns	1.8	-0.5
	TDL-E 360 ns	1.7	-0.4
	TDL-D 1100 ns	1.8	-0.4
	TDL-E 1100 ns	2.0	-0.2
Capacity Gain (Mbps)		0.2	9.4
Gain in IoT case (Users)		1	47
Gain in Mobile Video case (Users)		0	5

Regarding the performance in the case of mobile receivers (TDMA (II) and LL), the advantages of the different configurations presented in TABLE IV are confirmed. In TABLE V, an in-depth analysis is carried out in terms of capacity and reliability for the unicast services, which are delivered in the LL in the case of P-NOMA. Each of the metrics presented in TABLE V, demonstrates the gain of P-NOMA over the TDMA configuration. The SNR threshold gain has very little variation over the different channels. As expected, the first P-NOMA configuration presents a reliability gain of 1.7 dB for the same capacity value. The second case offers 9.4 Mbps of capacity gain by assuming a similar reliability performance (0.6 dB of deterioration on the worst case). Overall, these P-NOMA cases present a wide range of transmission configurations.

Last rows of TABLE V also present a capacity gain comparison, but in this case in terms of satisfied users for different potential P-NOMA use cases: IoT services and mobile video delivery. For the first one, the characteristics defined in the Rel-13 (Narrow Band loT LTE) have been taken into account, where a maximum data rate of 200 kbps per user in downlink channels is allowed [24]. For the second use case, where unicast users will receive HD video content in their mobile or portable devices, a minimum data rate of 2 Mbps has been assumed [25]. From the capacity calculations presented in TABLE V, while TDMA supports 256 unicast

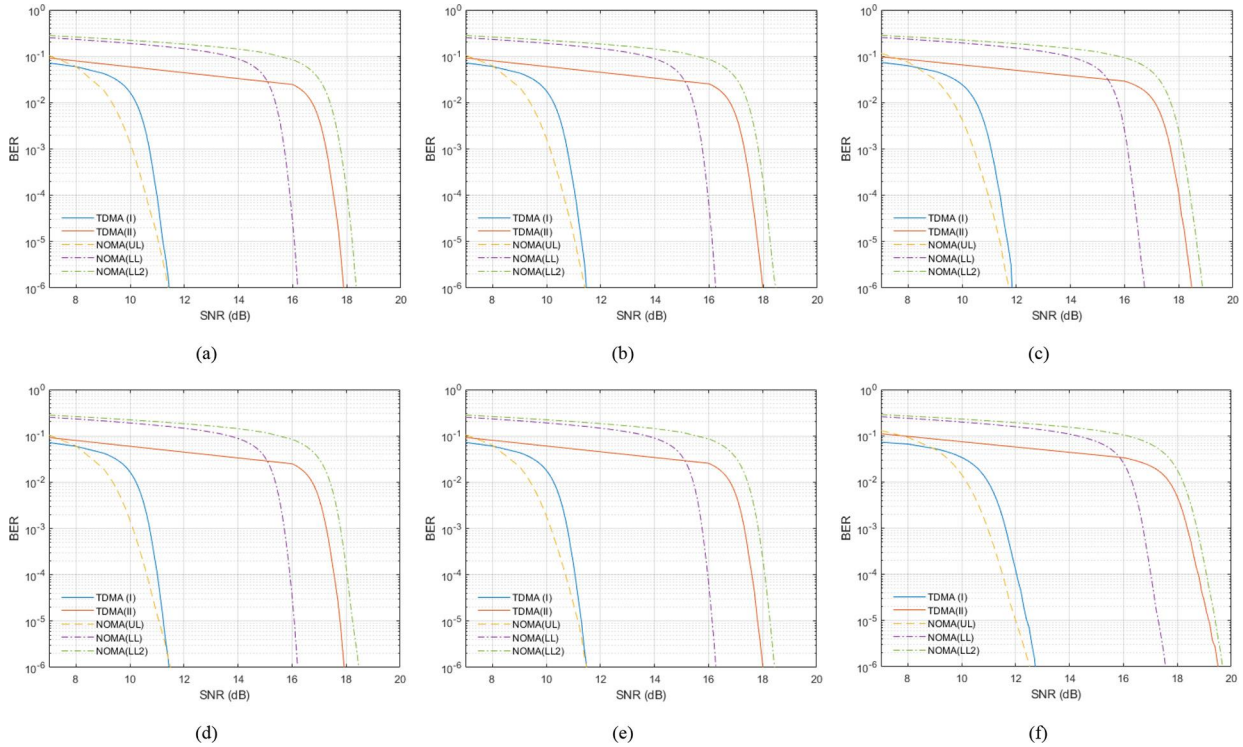

Fig. 5. Performance BER vs. SNR curves for different channel models: (a) TDL-D with 90 ns DDS, (b) TDL-D with 360 ns DDS, (c) TDL-D with 1100 ns DDS, (d) TDL-E with 90 ns DDS, (e) TDL-E with 360 ns DDS, (f) TDL-E with 1100 ns DDS.

users connected in the IoT case and 25 in the mobile video content delivery case, P-NOMA configurations increase considerably the amount of served users with up to 47 IoT devices and 5 mobile video devices.

VI. Network Simulation

The objective of this section is to test the performance of the proposed solution including MAC layer techniques and compare the performance with equivalent traditional TDMA solutions.

A. Simulation Methodology

The system evaluation has been carried out in an upgraded OMNeT++ [26]. This network simulation tool is composed of both PHY and MAC layers for each of the implemented transmitters and receivers. On the one hand, the PHY layer module facilitates the selection of the parameters that define the waveform. In addition, the transmission parameters have to be configured (modulation and code rate). PHY performance curves presented in the previous sections are used to estimate the transmission success. For each one of the received packets, the current SNR value of the receiver is used to determine the packet error rate (PER) according to the performance curves. The conversion from BER to PER is carried out following the technique presented in [27]. On the other hand, concerning the MAC layer, HARQ type retransmission schemes are implemented.

Regarding the network architecture and the implemented scenario, the channel model module and the mobility module are the most relevant parts of the simulated model. The former is in charge of defining the characteristics of the channel model, such as the Doppler frequency, the delay spread value or the implemented channel profile (TDL-D or TDL-E). Indeed, this module is closely related with the user type, since, while the channel for fixed receiver is considered almost constant, the channel affecting the receiver with the highest mobility will show a fastest change. This concept is also taken into account by the mobility model module, which takes care of detailing how the receiver is moving. Different mobility models are available in OMNeT++ for different type of receivers.

B. Network Setup

Three groups of users have been defined: fixed receivers, low-speed pedestrian receivers and car-mounted receivers. The first group of users represents traditional broadcast receivers, based on roof top antenna reception. However, pedestrian and car-mounted receivers will typically request more challenging data applications, e.g., on-demand video content. Therefore, this network architecture emulates a real scenario where a convergence application is required in order to guarantee the correct reception of broadcast and different unicast services.

In each simulation, a total number of 100 devices have been included. Specifically, 75 fixed receivers have been assumed inside each cell, 15 pedestrians and 10 car-mounted user devices. Fixed receivers have a static model, whereas pedestrians have been allocated a concrete walker mobility type referred as Random Way Point (RWP) [28]. In the case of cars, considering the characteristics of city roads, a linear mobility type has been used [29]. Speed is also specified for each

TABLE VI
SIMULATION PARAMETERS

Parameter	Value
Center Frequency	2 GHz
Tx Power	44 dBm
SCS	15 kHz
Distance attenuation	128.1 + 37.6*log(d)
Type of nodes	Fixed, pedestrians, cars
Speed	Fixed: 0 km/h Pedestrians: 3 km/h Cars: 30, 50 km/h
Number of Users	Fixed: 75 Pedestrians: 15 Cars: 10
Mobility type	Fixed: Static Pedestrians: RWP Cars: Linear
Inter-Site Distance (ISD)	500 m
Tx configuration (TDMA)	Broadcast: MCS12 Unicast: MCS19 Time division: 50%-50%
Tx configuration (NOMA)	Broadcast: MCS5 Unicast: MCS10, 12 IL: -6 dB
Desired Delay Spread	90, 360, 1100 ns
Noise Power	-90 dBm
Noise Figure	9 dB
Channel model	TDL-D, TDL-E
Simulated seeds	25
Simulation time	5 min per seed

receiver. Pedestrian receivers walk inside the cell with a mean speed of 3 km/h, and the car receivers vary their speed between 30-50 km/h.

The parameters values are critical when defining the propagation attenuation suffered by the transmitted signal. In this case, all the propagation channels presented in Fig. 5, based on TDL-D and TDL-E, have been considered with specific Doppler frequency values depending on the speed of the receiver.

The rest of the network simulation parameters are gathered in TABLE VI.

C. Results

The evaluation of the proposed NOMA-based 5G model has been based on three KPIs: reliability, latency and throughput. First, to measure the reliability, PER is used as a metric. Second, the user plane latency is evaluated. According to [30], user plane latency is defined as the required time to deliver a data packet between the Next Generation NodeB (gNB) and the user equipment (UE). The user plane latency can be modelled as:

$$T_{UP} = \tau_1 + p(\tau_2 + \tau_3) \tag{6}$$

where, p is the probability of requiring a retransmission, τ_1 is the transmission time, τ_2 is the HARQ request process time and τ_3 is the retransmission time. The complete process to calculate τ_1, τ_2 and τ_3 is obtained from [31]. The user plane latency is defined by the processing time at the UE ($t_{UE,rx}$). P-NOMA increases latency because the UE processing time will be higher (SIC module). In this case, following the complexity analysis of P-NOMA receivers carried out in [5], it is assumed that the $t_{UE,rx}$ increase in a two-layer system is 10% in comparison with a LL only case. Therefore, the minimum user plane latency that can be obtained is lower in the TDMA configuration than in the NOMA configuration, 1.785 ms vs. 1.796 ms, respectively. Moreover, the user plane latency deviation is also used in order to measure the latency variation with respect to the achievable minimum latency value. Finally, for the throughput, two metrics are used: normalized data reception index (NDRI) and effective throughput. The NDRI indicates the relation between the amount of information received and the maximum information rate that could be received in the error free case. Moreover, not only error packets reduce the NDRI value, also the delivered retransmissions, since using retransmissions, the overall received capacity is decreased because the same content is repeatedly transmitted. This parameter is measured in percentage data. The following expression has been used to calculate the NDRI:

$$NDRI\ (\%) = \frac{correct\ packets}{correct\ packets + retx\ attempts} \cdot 100 \tag{7}$$

where, *retx attempts* are the total number of retransmissions that have been carried out for each node. On the other hand, the effective throughput represents the useful received capacity. This parameter also takes into account the number of retransmissions that have been implemented by combing the NDRI with the transmitted capacity:

$$eff.throughput\ (Mbps) = \frac{NDRI \cdot tx\ capacity}{100} \tag{8}$$

In TABLE VII, a dual comparison of reliability and latency is presented between P-NOMA and TDMA configurations. Fixed receivers (UL) show equal PER values and user plane latency is also the same as no retransmissions are available for those users. User plane latency is the same for TDMA and NOMA cases, since being the service a broadcast type service, there is no uplink to transmit the feedback and, so, retransmissions cannot be implemented. In the case of mobile receivers, in general, the best reliability results are obtained in the NOMA (I) case, which is designed to improve the reliability. PER is reduced by 40% with respect to TDMA. As expected, NOMA (II) presents worse PER values than TDMA configuration. If the reliability is compared between different groups of users, the best results are for fixed receivers because they require lower SNR thresholds. In the case of mobile receivers, car-mounted ones show better behavior for their higher Doppler variation, that will make retransmissions more effective.

In TABLE VII, user plane latency values and deviations are presented. Although NOMA-based receivers have to cope with a latency penalization due to the SIC module, the lowest latency values appear in NOMA (I) because the reliability increase that the configuration offers compensates the latency penalization. In addition, user plane latency values are below 4 ms, which is the user plane latency requirement defined in [31] for eMBB applications. Therefore, all the presented cases meet the latency requirements. Moreover, car receivers have lower user plane latency values than pedestrians. High latency values indicate that more retransmissions

TABLE VII
NETWORK LEVEL RELIABILITY/LATENCY ANALYSIS

User Type	PER			User Plane Latency (ms)			User Plane Latency Deviation (μs)		
	TDMA	NOMA (I)	NOMA (II)	TDMA	NOMA (I)	NOMA (II)	TDMA	NOMA (I)	NOMA (II)
Fixed (UL)	$3.75 \cdot 10^{-5}$	$3.75 \cdot 10^{-5}$	$3.75 \cdot 10^{-5}$	1.785	1.785	1.785	-	-	-
Pedestrian (LL)	$6.13 \cdot 10^{-2}$	$3.66 \cdot 10^{-2}$	$7.14 \cdot 10^{-2}$	1.908	1.870	1.940	122.519	73.473	143.477
Car (LL)	$2.98 \cdot 10^{-2}$	$1.75 \cdot 10^{-2}$	$3.47 \cdot 10^{-2}$	1.845	1.831	1.866	59.620	35.193	69.737
Total	$1.22 \cdot 10^{-2}$	$7.26 \cdot 10^{-3}$	$1.42 \cdot 10^{-2}$	1.883	1.854	1.910	97.360	58.161	113.981

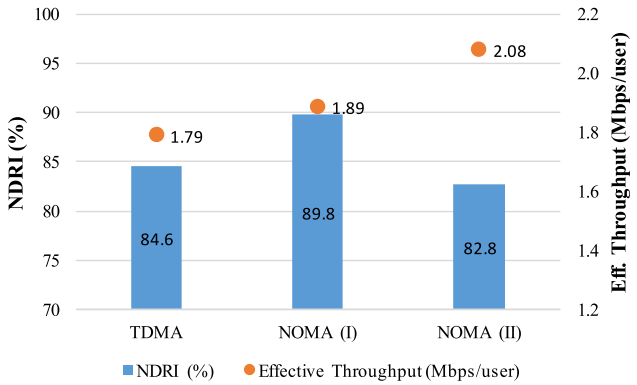

Fig. 6. Network level throughput analysis of the LL (unicast services).

are needed for a proper decoding than in cases with low latency. Therefore, latency results confirm that retransmissions are more effective in the case of cars, while in the case of pedestrians have lower effect. Regarding user plane latency deviation results, NOMA (I) case presents the lowest values, which indicates that the calculated user plane latency is closer to minimum than in any other case. This effect makes NOMA (I) even more interesting as it provides higher degree of determinism.

Fig. 6 shows only mobile receiver throughput (fixed receivers show identical behavior). Looking at the NDRI, the results are equivalent to PER values. NOMA (I) outperforms NOMA (II) and TDMA. If effective throughput is considered, TDMA offers the worst behavior (below 1.8 Mbps/user), while NOMA cases increment the effective throughput when increasing the implemented MCS. The difference between TDMA and the best case (NOMA (II)) is an increment of 14%. These results indicate that the reliability decrease is compensated by transmitting with a higher capacity configuration.

VII. CONCLUSION

This paper proposes a PHY/MAC enabler solution for broadcast and unicast convergence in 5G NR. The solution is based on Power domain Non Orthogonal Multiple Access (P-NOMA). The system configuration parameters have been analyzed, and different configuration options have been discussed. For instance, the IL has been identified as a key configuration parameter for the broadcast/unicast convergence use case since introduces an additional multiplexing variable that provides a wider flexibility range. This flexibility has been used to increase the reliability of the unicast receivers and to deliver higher data rate to the unicast receivers.

A system transceiver prototype has been design and implemented for testing purposes. Two different evaluation procedures have been developed to obtain the system performance from various perspectives. In the PHY layer analysis, different P-NOMA-based configurations have been defined in order to cover a specific service convergence use case, namely NOMA (I) and NOMA (II). Based on these configurations, possible reliability and/or capacity gains were foreseen first, and then, confirmed by using different AWGN and TDL channel models. In the case of the capacity gain, depending on the configuration used, up to 47 IoT receivers and 5 mobile video receivers could be added to the network. The system level performance has been analyzed using a network simulation environment. Reliability, latency and throughput have been evaluated by using different metrics. Reliability and latency measurements indicate that the most appropriate configuration for those terms for the unicast services is NOMA (I). However, from the capacity perspective, NOMA (II) is the best solution because it offers the highest capacity per user rate. Moreover, HARQ retransmission schemes appear to be more effective when the receivers are moving faster, due to the higher channel response variance. All in all, based on the obtained results, NOMA can be considered as a competitive alternative broadcast/unicast convergence.

There are still some future works on the horizon. On the one hand, concerning the stack protocol, upper layers should be taken into account for future developments. For example, if the network layer is included in addition to the proposed service level convergence, IP-based convergence could also be proposed. In this case, 5G NR could be combined with another technology, such as ATSC 3.0 or DVB-T2. On the other hand, as highlighted in Section V-B, one of the proposed NOMA configurations provides a considerable reliability gain that could be transformed in coverage area improvement. Therefore, similar configurations could be used in rural areas or isolated small areas presenting limitations on the service quality. Finally, new resource management strategies could be combined with this solution. Interesting candidate alternatives are subgrouping techniques based on the architecture proposed in [15].

REFERENCES

[1] *Cisco Visual Networking Index: Global Mobile Data Traffic Forecast Update, 2016–2021*, Cisco, San Jose, CA, USA, 2017.
[2] *NR; Physical Layer; General Description, Technical Specification Group Services and System Aspects V15.0.0*, Standard TS 38.201, Jan. 2018.
[3] "IMT vision—Framework and overall objectives of the future development of IMT for 2020 and beyond," ITU, Geneva, Switzerland, ITU Recommendation M.2083-0, Sep. 2015.
[4] L. Zhang *et al.*, "Layered-division-multiplexing: Theory and practice," in *IEEE Trans. Broadcast.*, vol. 62, no. 1, pp. 216–232, Mar. 2016.
[5] S. I. Park *et al.*, "Low complexity layered division multiplexing for ATSC 3.0," *IEEE Trans. Broadcast.*, vol. 62, no. 1, pp. 233–243, Mar. 2016.

[6] L. Fanari *et al.*, "Trends and challenges in broadcast and broadband convergence," in *Proc. IEEE Int. Conf. Elect. Eng. Photon. (EExPolytech)*, St Petersburg, Russia, 2019, pp. 153–156.
[7] D. Lecompte and F. Gabin, "Evolved multimedia broadcast/multicast service (eMBMS) in LTE-advanced: Overview and Rel-11 enhancements," *IEEE Commun. Mag.*, vol. 50, no. 11, pp. 68–74, Nov. 2012.
[8] C. Hoymann *et al.*, "LTE release 14 outlook," *IEEE Commun. Mag.*, vol. 54, no. 6, pp. 44–49, Jun. 2016.
[9] A. Ghosh, A. Maeder, M. Baker, and D. Chandramouli, "5G evolution: A view on 5G cellular technology beyond 3GPP release 15," *IEEE Access*, vol. 7, pp. 127639–127651, 2019.
[10] D. Ratkaj and A. Murphy, Eds., *Definition of Use Cases, Requirements and KPIs, Deliverable D2.1*, 5G-PPP 5G-Xcast project, Oct. 2017.
[11] J. J. Gimenez *et al.*, "5G new radio for terrestrial broadcast: A forward-looking approach for NR-MBMS," *IEEE Trans. Broadcast.*, vol. 65, no. 2, pp. 356–368, Jun. 2019.
[12] D. Gomez-Barquero, D. Navratil, S. Appleby, and M. Stagg, "Point-to-multipoint communication enablers for the fifth generation of wireless systems," *IEEE Commun. Stand. Mag.*, vol. 2, no. 1, pp. 53–59, Mar. 2018.
[13] L. Zhang, Y. Wu, W. Li, K. Salehian, A. Florea, and G. K. Walker, "Improving LTE eMBMS system spectrum efficiency and service quality using channel bonding, non-orthogonal multiplexing and SFN," in *Proc. IEEE Int. Symp. Broadband Multimedia Syst. Broadcast. (BMSB)*, Nara, Japan, 2016, pp. 1–8.
[14] L. Zhang *et al.*, "Layered-division multiplexing: An enabling technology for multicast/broadcast service delivery in 5G," *IEEE Commun. Mag.*, vol. 56, no. 3, pp. 82–90, Mar. 2018.
[15] J. Montalban *et al.*, "Multimedia multicast services in 5G networks: Subgrouping and non-orthogonal multiple access techniques," *IEEE Commun. Mag.*, vol. 56, no. 3, pp. 91–95, Mar. 2018.
[16] J. Zhao, D. Gündüz, O. Simeone, and D. Gómez-Barquero, "Non-orthogonal unicast and broadcast transmission via joint beamforming and LDM in cellular networks," *IEEE Trans. Broadcast.*, submitted for publication.
[17] L. Zhang *et al.*, "Using non-orthogonal multiplexing in 5G-MBMS to achieve broadband-broadcast convergence with high spectral efficiency," *IEEE Trans. Broadcast.*, vol. 66, no. 2, Jun. 2020.
[18] E. Iradier, J. Montalban, D. Romero, Y. Wu, L. Zhang, and W. Li, "NOMA based 5G NR for PTM communications," in *Proc. IEEE Int. Symp. Broadband Multimedia Syst. Broadcast. (BMSB)*, 2019, pp. 1–6.
[19] L. Michael and D. Gómez-Barquero, "Bit-interleaved coded modulation (BICM) for ATSC 3.0," *IEEE Trans. Broadcast.*, vol. 62, no. 1, pp. 181–188, Mar. 2016.
[20] S. Ahn, K. Kim, S. Myung, S. Park, and K. Yang, "Comparison of low-density parity-check codes in ATSC 3.0 and 5G standards," *IEEE Trans. Broadcast.*, vol. 65, no. 3, pp. 489–495, Sep. 2019.
[21] "Study on channel model for frequencies from 0.5 to 100 GHz," 3GPP, Sophia Antipolis, France, Rep. TR 38.901, 2017.
[22] *Service Requirements for the 5G System; Stage 1, V15.7.0, Release. 15, Technical Specification Group Services and System Aspects*, Standard 3GPP TS 22.261, Dec. 2018.
[23] *NR; Physical Layer Procedures for Data (Release 15), V15.3.0, Technical Specification Group Services and System Aspects*, Standard 3GPP TS 38.214, Sep. 2018.
[24] S. Persia and L. Rea, "Next generation M2M cellular networks: LTE-MTC and NB-IoT capacity analysis for smart grids applications," in *Proc. AEIT Int. Annu. Conf. (AEIT)*, 2016, pp. 1–6.
[25] X. Xu, J. Liu, and X. Tao, "Mobile edge computing enhanced adaptive bitrate video delivery with joint cache and radio resource allocation," *IEEE Access*, vol. 5, pp. 16406–16415, 2017.
[26] A. Varga and R. Hornig, "An overview of the OMNET++ simulation environment," in *Proc. 1st Int. Conf. Simulat. Tools Tech. Commun. Netw. Syst. Workshops (ICST)*, 2008, p. 60.
[27] Z. Li *et al.*, "A cross-layer design for wireless VoIP: Playout delay constrained ARQ with ARQ aware adaptive playout buffer," in *Advances in Network and Communications Engineering*, 2004, p. 11.
[28] E. Hyytia, H. Koskinen, P. Lassila, and A. Penttinen, "Random waypoint model in wireless networks," in *Networks and Algorithms: Complexity in Physics and Computer Science*, Jun. 2005.
[29] O. G. Olaleye, A. Ali, D. Perkins, and M. Bayoumi, "Modeling and performance simulation of PULSE and MCMAC protocols in RFID-based IoT network using OMNeT++," in *Proc. IEEE Int. Conf. RFID (RFID)*, Orlando, FL, USA, 2018, pp. 1–5.
[30] "Study on scenarios and requirements for next generation access technologies, v15.0.0," 3GPP, Sophia Antipolis, France, Rep. TR 38.913, Jun. 2018.
[31] E. Garro *et al.*, "5G mixed mode: NR multicast-broadcast services," *IEEE Trans. Broadcast.*, vol. 66, no. 2, Jun. 2020.

Eneko Iradier (Student Member, IEEE) received the B.Sc. and M.Sc. degrees in telecommunications engineering from the University of the Basque Country (UPV/EHU) in 2016 and 2018, respectively, where he is currently pursuing the Ph.D. degree. Since 2015, he has been part of the TSR Research Group, UPV/EHU. He was with the Communications Systems Group of IK4-Ikerlan as a Researcher from 2017 to 2018. During his doctoral studies, he did an internship at Communications Research Centre Canada, Ottawa. His current research interests include the design and development of new technologies for the physical layer of communication systems and broadcasting in 5G environments.

Jon Montalban (Member, IEEE) received the M.S. and Ph.D. degrees in telecommunications engineering from the University of the Basque Country, Spain, in 2009 and 2014, respectively. He is part of the Radiocommunications and Signal Processing Research Group, University of the Basque Country, where he is an Assistant Professor involved in several research projects. He has hold visiting research appointments with the Communication Research Centre, Canada, and Dublin City University, Ireland. His current research interests are in the area of wireless communications and signal processing for reliable industrial communications. He is the co-recipient of several best paper awards including the Scott Helt Memorial Award to Recognize the Best Paper Published in the IEEE TRANSACTIONS ON BROADCASTING in 2019. He has served as a reviewer for several renowned international journals and conferences in the area of wireless communications and currently serves as an Associate Editor for IEEE ACCESS.

Lorenzo Fanari (Student Member, IEEE) received the B.Sc. degree in electrical and electronic engineering and the M.Sc. degree in telecommunication engineering from the University of Cagliari, Italy, in 2015 and 2018, respectively. He is currently pursuing the Ph.D. degree with the University of the Basque Country, Spain. His research interests include coding theory and wireless communications.

Pablo Angueira (Senior Member, IEEE), received the M.S. and Ph.D. degrees in telecommunication engineering from the University of the Basque Country, Spain, in 1997 and 2002 respectively.

He joined the Communications Engineering Department, University of the Basque Country in 1998, where he is currently a Full Professor. He is part of the staff of the Signal Processing and Radiocommunication Lab (http://www.ehu.es/tsr), where he has been involved in research on digital broadcasting (DVB-T, DRM, T-DAB, DVB-T2, DVB-NGH, and ATSC 3.0) for more than 20 years. He has coauthored an extensive list of papers in international peer-reviewed journals, and a large number of conference presentations in digital broadcasting. He has also coauthored several contributions to the ITU-R working groups WP6 and WP3. His main research interests are network planning and spectrum management applied to digital terrestrial broadcast technologies. He is currently involved in research activities related to broadcasting in a 5G environment.

Prof. Angueira is an Associate Editor of the IEEE TRANSACTIONS ON BROADCASTING, a member of the IEEE BMSB International Steering Committee and a Distinguished Lecturer of the IEEE Broadcast Technology Society. He serves on the Administrative Committee for the IEEE Broadcast Technology Society.

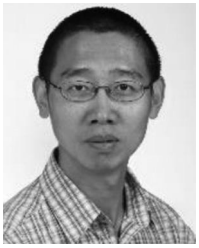

Liang Zhang (Senior Member, IEEE) received the bachelor's degree from the Department of Electronic Engineering and Information Science, University of Science and Technology of China, Hefei, China, in 1996, and the M.S. and Ph.D. degrees from the Department of Electrical and Computer Engineering, University of Ottawa, Ottawa, ON, Canada, in 1998 and 2002, respectively. He is a Senior Research Scientist with the Communications Research Centre Canada, Ottawa. He has been deeply involved in the ATSC 3.0 standardization activities on developing the layered-division-multiplexing technology, mixed fixed and mobile broadcast service delivery, mobile service detection, co-channel interference mitigation, integrated access and backhaul. He is currently working on technologies for the convergence of future TV broadcast and 5G broadband systems. He has more than 70 peer-reviewed Journal and conference publications and received the Multiple Best Paper Awards from IEEE, IBC, and NAB for his work on the Next Generation ATSC 3.0 and the 5G Broadcasting Systems. He is an Associate Editor of the IEEE TRANSACTIONS ON BROADCASTING and IEEE Broadcast Technology Society Distinguished Lecturer, and the elected member of the IEEE Broadcast Technology Society Administrative Committee.

Yiyan Wu (Fellow, IEEE) received the M.Eng. and Ph.D. degrees in electrical engineering from Carleton University, Ottawa, ON, Canada, in 1986 and 1990, respectively.

He is a Principal Research Scientist with the Communications Research Centre Canada. He is an Adjunct Professor with Carleton University and Western University, Canada. He has more than 400 publications. His research interests include broadband multimedia communications, digital broadcasting, and communication systems engineering. He received many technical awards for his contribution to the research and development of digital broadcasting and broadband multimedia communications. He is a Distinguished Lecturer of the IEEE Broadcast Technology Society, and a member of the ATSC Board of Directors, representing IEEE. He was appointed as a Member of the Order of Canada in 2018. He is a Fellow of the Canadian Academy of Engineering.

Wei Li (Member, IEEE) received the B.E. degree in electrical engineering from Shandong University in 1985, the M.S. degree in electrical engineering from the University of Science and Technology of China, in 1988, and the Ph.D. degree in electrical engineering from the Institut National des Sciences Appliquées of Rennes, France, in 1996. In 2001, he joined Communications Research Centre Canada (CRC), where his major focus is broadband multimedia systems and digital television broadcasting. He is currently a Research Scientist with CRC. He served as the Session Chair for the IEEE International Symposium on Broadband Multimedia Systems and Broadcasting in 2006, 2007, 2015, 2016, and the TPC Chair in 2016. He was the Managing Editor of the IEEE TRANSACTIONS ON BROADCASTING Special Issue on IPTV in Broadcasting Applications in 2009. He also served as a reviewer for several renowned international journals and conferences in the area of broadcasting, multimedia communication, and multimedia processing. He was the BTS IPTV representative at the ITU-T and the Co-Chair of Enhanced TV Planning Team at ATSC. He is the Associate Editor of the IEEE TRANSACTIONS ON BROADCASTING and IEEE ACCESS.